Minimally modified human blood coagulation factor X to bypass direct factor Xa inhibitors

Schreuder, M.; Jourdi, G.; Veizaj, D.; Poole, D.A. .I.I.I.; Cheung, K.L.; Poenou, G.; ... ; Bos, M.H.A.

Received: 30 October 2023 | Revised: 9 April 2024 | Accepted: 23 April 2024

https://doi.org/10.1016/j.jtha.2024.04.022

ORIGINAL ARTICLE

Minimally modified human blood coagulation factor X to bypass direct factor Xa inhibitors

Mark Schreuder[1] | Georges Jourdi[2,3,4] | Dejvid Veizaj[1] | David A. Poole III[5] | Ka Lei Cheung[1] | Géraldine Poenou[1,3] | Daniël Verhoef[1,6] | Stella Thomassen[7] | Laura F. H. Janssen[5] | Alain Stepanian[4,8] | Tilman M. Hackeng[7] | Pascale Gaussem[3,9] | Pieter H. Reitsma[1,6] | Daan P. Geerke[5] | Virginie Siguret[3,4] | Mettine H. A. Bos[1]

[1]Department of Internal Medicine, Division of Thrombosis and Hemostasis, Einthoven Laboratory for Vascular and Regenerative Medicine, Leiden University Medical Center, Leiden, The Netherlands

[2]Assistance publique – Hôpitaux de Paris (AH-HP) Centre, Service d'hématologie biologique, Hôpital Cochin, Paris, France

[3]Innovative Therapies in Haemostasis, Institut national de la santé et de la recherche médicale (INSERM) U1140, Université Paris Cité, Paris, France

[4]Assistance publique – Hôpitaux de Paris (AH-HP) Nord, Service d'hématologie biologique, Hôpital Lariboisière, Paris, France

[5]Amsterdam Institute of Molecular and Life Sciences (AIMMS), Division of Molecular and Computational Toxicology, Department of Chemistry and Pharmaceutical Sciences, Vrije Universiteit Amsterdam, Amsterdam, The Netherlands

[6]VarmX B.V., Leiden, The Netherlands

[7]Department of Biochemistry, Cardiovascular Research Institute Maastricht, Maastricht University, Maastricht, The Netherlands

[8]EA3518 Institut Universitaire d'Hématologie, Hôpital Saint Louis, Paris-Diderot, Paris, France

[9]Assistance publique – Hôpitaux de Paris (AP-HP) Centre, Service d'hématologie biologique, Hôpital Européen Georges Pompidou, Paris, France

Abstract

Background: Direct oral factor (F)Xa inhibitors are widely used as alternatives to conventional vitamin K antagonists in managing venous thromboembolism and non-valvular atrial fibrillation. Unfortunately, bleeding-related adverse events remain a major concern in clinical practice. In case of bleeding or emergency surgery, rapid-onset reversal agents may be required to counteract the anticoagulant activity.

Objectives: The ability of FXa variants to bypass the direct oral FXa inhibitors was assessed.

Methods: Human FXa variants were generated through substitution of phenylalanine 174 (F174) for either alanine, isoleucine, or serine. FXa variants were stably expressed in HEK293 cells and purified to homogeneity using ion-exchange chromatography.

Results: F174-substituted human FX variants demonstrated efficacy in restoring thrombin generation in plasma containing direct FXa inhibitors (apixaban, rivaroxaban, edoxaban). Their ability to bypass the anticoagulant effects stems from a significantly reduced sensitivity for the direct FXa inhibitors due to a decrease in binding affinity determined using molecular dynamics simulations and free energy computation. Furthermore, F174 modification resulted in a partial loss of inhibition by tissue factor pathway inhibitor, enhancing the procoagulant effect of F174-substituted FX. Consequently, the F174A- and F174S-substituted FX variants effectively counteracted the effects of 2 widely used anticoagulants, apixaban and rivaroxaban, in plasma of atrial fibrillation and venous thromboembolism patients.

Conclusion: These human FX variants have the potential to serve as a rescue reversal strategy to overcome the effect of direct FXa inhibitors in case of life-threatening bleeding events or emergency surgical interventions.

Manuscript handled by: Patricia Liaw

Final decision: Patricia Liaw, 23 April 2024

Georges Jourdi and Dejvid Veizaj contributed equally to this study.

Correspondence Mettine H. A. Bos, Department of Internal Medicine, Division of Thrombosis and Hemostasis, Einthoven Laboratory for Vascular and Regenerative Medicine, Leiden University Medical Center, Albinusdreef 2, 2333 ZA, Leiden, The Netherlands.
Email: M.H.A.Bos@lumc.nl

Present address
Mark Schreuder, The Centenary Institute, University of Sydney, Camperdown, New South Wales, Australia.

Funding information
This work was financially supported by the Landsteiner Foundation for Blood Transfusion (LSBR, grant number 1451) and the PPS Allowance Health~Holland, Top Sector Life Sciences & Health. The funding agencies had no role in the preparation, review, or approval of the manuscript.

KEYWORDS
anticoagulants, antidotes, factor Xa inhibitors, hemorrhage, molecular dynamics simulation

1 | INTRODUCTION

Thromboembolic events contribute significantly to morbidity with a global incidence rate of 2000 cases per 100 000 and have been estimated to account for 1 in 4 deaths, representing a leading cause of mortality worldwide [1]. Individuals with a heightened tendency to form thrombi are at increased risk of ischemic heart disease, stroke, deep-vein thrombosis, pulmonary embolism, and other cardiovascular disorders. The direct oral anticoagulants (DOACs) targeting the key coagulation protease factor (F)Xa [2–5] or thrombin [6] are widely used in the management and prevention of thrombotic events [7]. However, major bleeding complications are observed in 1% to 5% of DOAC-treated patients [8–10]. Considering that these anticoagulants are prescribed to millions of people worldwide, anticoagulant-associated bleeding is a prominent clinical concern [11,12]. Life-threatening or uncontrollable bleeding requires the use of agents that enable rapid reversal of the anticoagulant activity [13,14]. With the direct FXa inhibitors representing the vast majority of DOAC prescriptions [15,16], access to an effective reversal agent for the direct FXa inhibitors is of critical importance. Currently, andexanet alfa (andexanet) [17] is the only US Food and Drug Administration and European Medicines Agency–approved specific reversal agent for the direct FXa inhibitors. Andexanet has proven to be effective for the treatment of direct FXa inhibitor-related bleeding, achieving excellent or good hemostasis in 82% of patients treated in the Andexanet Alfa, a Novel Antidote to the Anticoagulation Effects of FXa Inhibitors (ANNEXA)-4 study [17] and demonstrating superior hemostatic efficacy compared with usual care in the ANNEXA-I trial [18]. In both studies, thrombotic events occurred in 10% of the patients within 30 days following andexanet treatment [17,18]. In contrast, fewer thrombotic events were observed following treatment with other reversal agents, such as prothrombin complex concentrate for reversal of the FXa inhibitors apixaban or rivaroxaban (3%-8%) [19–21], idarucizumab-mediated reversal of dabigatran (5%) [22], or vitamin K antagonist reversal (4%-7%) [23,24]. The relatively high incidence of venous thrombosis in andexanet-treated patients is associated with the sequestering of the natural anticoagulant tissue factor pathway inhibitor (TFPI) following interaction with andexanet [25,26]. Although it is unlikely that andexanet interacts with TFPI when bound to a direct FXa inhibitor, the administered high dose of andexanet could generate a significant circulating pool of antidote in free form that would allow for a direct interaction with TFPI, thereby preventing TFPI from interacting with endogenous FXa.

Andexanet is one of the several FXa-based reversal agents that have originated from bioengineering of FXa and function either by sequestering or bypassing direct FXa inhibitors [27]. Andexanet is a catalytically inactive gamma-carboxy glutamic acid (Gla)-domainless FXa that functions as a decoy by stoichiometric binding of the inhibitors in order to restore endogenous thrombin generation [28]. Yet, the active site residues and exosites remain available for potential interactions with pro- and anticoagulant proteins [25,26,29,30]. To prevent such macromolecular interactions, Jourdi et al. [31,32] generated a Gla-domainless FXa sequestered by α_2-macroglobulin (GDFXa-α_2M), which retains its affinity for the direct FXa inhibitors. Alternatively, a zymogen-like FXa variant (FXa-I16L) demonstrating impaired binding of FXa inhibitors has been explored as prohemostatic bypassing agent [33,34]. Recently, we reported a FX variant comprising an extended 99-loop (FX-C) that sterically hinders interactions with the direct FXa inhibitors [35]. Using molecular dynamics (MD) simulations, we showed that residues Y99, F174, and W215 that form the S4 subsite region in the FXa active site (Supplementary Figure S1) have stabilizing contacts with the bound FXa inhibitor apixaban. Note that chymotrypsinogen residue numbering will be used throughout the manuscript, and these 3 residues are Y279, F356, and W399 in the mature FX sequence, respectively. With partially purified FXa preparations, we

demonstrated that disruption of the S4 subsite through alanine-substitution of Y99 and/or F174 resulted in a more than 10-fold loss of apixaban sensitivity [35]. As Y99-substituted FXa showed a dramatic loss in FXa clotting activity, F174-substituted FXa displayed the potential to restore the anticoagulant effects of the direct FXa inhibitors.

In this report, we explored the ability of purified F174-substituted FX(a) variants to facilitate thrombin generation in the presence of the direct FXa inhibitors. Our *in vitro* data demonstrate that these FXa variants exhibit a reduced sensitivity for the natural inhibitor TFPI and for the direct FXa inhibitors. Using standard MD approaches, we demonstrated that these FXa variants feature a lower binding affinity for apixaban due to the F174 substitutions. Furthermore, the F174-substituted FX variants restored thrombin generation in plasma derived from atrial fibrillation and venous thrombosis patients treated with apixaban or rivaroxaban. These studies demonstrate that F174-substituted FX variants have the potential to serve as an alternative therapeutic option to counteract bleeding induced by direct FXa inhibitors.

2 | MATERIALS AND METHODS

2.1 | Materials

Apixaban (Adooq Bioscience) was dissolved to 5 mg/mL (10.9 mM) in a vehicle (10% ethanol, 10% glycerol, 10% PEG400, 3.5% dextrose [v/v]). Rivaroxaban and edoxaban (10 mM in dimethyl sulfoxide) were from Hölzel Diagnostika. The peptidyl substrate methoxycarbonylcyclohexyl-Gly-Gly-Arg-pNA (SpecXa) was from Sekisui Diagnostics, and N-α-benzyloxycarbonyl-D-Arg-Gly-Arg-pNA (S2765) and H-D-Phe-Pip-Arg-pNA (S2238) were from Instrumentation Laboratories. All tissue culture reagents were from Life Technologies. Calibrator (Thrombin Calibrator) and fluorescent substrate (FluCa) were from Thrombinoscope. FX-depleted human plasma, prothrombin time (PT) reagent (Neoplastine CI Plus), and activated partial thromboplastin time (APTT) reagent (Triniclot) were from Stago. Normal pooled plasma was from Sanquin. Unfractionated heparin (UFH) was from LEO Pharma. Small unilamellar phospholipid vesicles (PCPS) composed of 75% (wt/wt) hen egg L-phosphatidylcholine and 25% (wt/wt) porcine brain L-phosphatidylserine (Avanti Polar Lipids) were prepared and characterized as described [36]. All functional assays were performed in HEPES-buffered saline (HBS; 20 mM HEPES, 0.15 M NaCl, pH 7.5) supplemented with 5 mM $CaCl_2$, 0.1% PEG8000 filtered over a 0.2 μm filter (assay buffer).

2.2 | DOAC patient plasma

Blood samples from 89 patients (male/female, 56%/44%; mean age, 62 ± 8 years) treated with direct FXa inhibitors were collected from Cochin and Lariboisière University Hospitals (Assistance Publique – Hôpitaux de Paris, Paris, France). Forty-seven patients were treated for non-valvular atrial fibrillation (23 with apixaban; 24 with rivaroxaban) and 54 for venous thromboembolic disease (27 with apixaban; 27 with rivaroxaban). Patients gave their written informed consent, and the investigation was conducted according to the Declaration of Helsinki. Blood was collected in 0.109 M buffered trisodium citrate (9:1 v/v; Greiner Bio-One), and platelet-poor plasma was prepared following 2 sequential centrifugation steps at 2500 g for 15 minutes at room temperature and stored at −80 °C. Plasma was briefly thawed at 37 °C immediately prior to analysis; all assays were performed in a blinded manner and according to the manufacturers' assay instructions. Plasma concentrations of direct FXa inhibitors were assessed using a specific anti-Xa assay (STA Liquid Anti-Xa, Stago) on STAR Analysers (STAR evolution analyser, Stago) using dedicated calibrators and controls with a lower limit of quantification of 18 ng/mL. Fibrinogen levels were measured by the Clauss method (Dade Thrombin). PT results were expressed as international normalized ratio.

2.3 | Proteins

Human plasma-derived FV, FVIIa, FIXa, prothrombin, α-thrombin, antithrombin (AT), the inhibitor dansylarginine-N-(3-ethyl-1,5-pentanediyl)amide (DAPA), Russell's viper venom-X activator, and corn trypsin inhibitor were from Prolytix. r-TFPI (Tifacogin) was obtained from Novartis. Monoclonal inhibitory antibodies against the TFPI Kunitz 1 domain, the TFPI Kunitz 2 domain, or a mix of anti-Kunitz 1 domain, anti-Kunitz domain 2, and anti-TFPI C-terminus were obtained from Sanquin. Human tissue factor (TF, Innovin) was obtained from Siemens, and recombinant (r-)FVIII (NovoEight) was from Novo Nordisk. Recombinant constitutively active B-domainless human FV (FV-810) [37] was large-scale expressed in baby hamster kidney cells, conditioned media was collected, and the protein was purified as described [35].

2.4 | Construction, expression, and partial purification of FX variants

DNA constructs encoding FX variants comprising the Phe174Ala (FX-F174A) or Phe174Ser (FX-F174S) substitution were prepared from the pCMV4 vector carrying wild-type human FX [38] by site-directed mutagenesis using the Q5 Mutagenesis Kit (New England Biolabs). Transfection of the plasmids encoding the FX constructs into HEK293 cells, the selection of stable clones, and the expression and purification of the FX variants were performed as described previously [35]. Partially purified FX variants were obtained by expanding the stable cell line into three 175 cm^2 cell flasks and conditioning for 24 hours in FX-specific expression media. Conditioned media was collected for 3 consecutive days, centrifuged at 4000 g, filtered over a 0.45 μm polyethersulfone membrane, and supplemented with 1 mM benzamidine prior to storage at −20 °C. Following thawing of the conditioned media, the media was ultrafiltrated employing Amicon Ultra-15 centrifugal filter units (Merck) with 30 kDa molecular weight cutoff to ∼2 mL in HBS, 50% (v/v) glycerol, and stored at −20 °C.

2.5 | Purification of FXa

Purified r-FX and FX variants (FX-F174A and FX-F174S) were activated with Russell's viper venom-X (1.15 μg/mL FX), applied to a benzamidine sepharose 6B column (Cytiva) equilibrated in HBS and eluted using HBS supplemented with 4 mM benzamidine. Fractions were analyzed for FXa activity employing peptidyl substrate hydrolysis (SpecXa). Fractions containing FXa activity were pooled and precipitated by addition of 0.516 g/mL ammonium sulfate (Sigma Aldrich) by stirring and overnight incubation at 4 °C. The following day, samples were centrifuged at 10 000g for 30 minutes at 4 °C, and the supernatant was removed. Precipitate was dissolved to ~3 mg/mL in HBS containing 50% (v/v) glycerol and stored at −20 °C. Purified products were visualized by sodium dodecyl sulfate–polyacrylamide gel electrophoresis employing Coomassie Brilliant Blue staining.

2.6 | Specific FX activity

The specific extrinsic clotting activity was determined using a modified FX-specific PT-based assay. FX-depleted plasma (45 μL) was mixed with a 5 μL FX sample, followed by a 60-second incubation period at 37 °C. Coagulation was initiated with the addition of 50 μL PT reagent, and the coagulation time was monitored using a Start4 coagulation instrument (Stago). The specific intrinsic clotting activity was determined using a modified FX-specific APTT-based assay. FX-depleted plasma (45 μL) was mixed with FX sample (5 μL) and APTT reagent (50 μL), followed by a 180-second incubation period at 37 °C. Coagulation was initiated with the addition of 50 μL of 25 mM $CaCl_2$, upon which the coagulation time was monitored. Reference curves consisted of serial dilutions of normal pooled plasma that were employed to convert clotting times to U/mg, assuming 1 U/mL FX in normal pooled plasma equals 9 μg/mL FX.

2.7 | Macromolecular substrate activation

Steady-state initial velocities of macromolecular substrate cleavage were determined discontinuously at 25 °C in assay buffer as described [39,40]. Briefly, progress curves of prothrombin activation were obtained by incubating PCPS (50 μM), DAPA (10 μM), and prothrombin (1.4 μM) with r-FV-810 (20 nM), and the reaction was initiated with 0.1 to 0.4 nM of r-FXa, FXa-F174A, or FXa-F174S upon which the rate of prothrombin conversion was measured. The kinetic parameters and equilibrium binding constants for prothrombin and cofactor Va (FV-810) were determined using increasing concentrations of respective proteins [39]. Prothrombin conversion was assayed in the absence or presence of the direct FXa inhibitors apixaban, rivaroxaban, or edoxaban (1 pM to 100 μM) in order to determine the half maximal inhibitory concentration (IC_{50}) concentrations for each prothrombinase-assembled FXa variant.

Inhibition by TFPI was assessed using 0 to 10 nM TFPI incubated with PCPS (50 μM), DAPA (10 μM), prothrombin (1.4 μM), and FV-810 (2 nM). Reactions were initiated with 0.05 nM FXa, and at selected time points (5-60 minutes), aliquots were taken and quenched in HBS supplemented with 50 mM EDTA buffer. The rate of prothrombin conversion was measured as described above and corrected for substrate consumption according to a previously established model system [41]. Inhibitory constant values were determined using normalized thrombin values at 30 minutes and subsequent analysis by linear regression.

The rate of FX (9.1-2500 nM) activation by the TF-FVIIa complex (TF 0.1 nM; FVIIa 0.5 nM) was determined in the presence of PCPS (50 μM) in assay buffer at 25 °C. At selected time points (0.5-4 minutes), aliquots were taken and quenched in EDTA buffer. The amidolytic activity of each sample was determined by SpecXa conversion (250 μM), and the initial rates of chromogenic substrate hydrolysis were converted to nanomolar of product by reference to a standard curve. The apparent K_M and k_{cat} values for substrate activation were calculated from the Michaelis–Menten equation. For FX activation by the FVIIIa-FIXa complex (FVIIIa 5 nM; FIXa 0.5 nM; PCPS 50 μM), a similar approach was used. FVIII (NovoEight; 40nM) was activated by thrombin (100 nM) for 30 seconds at 25 °C, and the reaction was stopped by the addition of a 10-fold molar excess of hirudin. FXa formation was assessed as described above.

2.8 | Chromogenic substrate hydrolysis

The kinetics of peptidyl substrate hydrolysis were measured in assay buffer using increasing concentrations of SpecXa (10-600 μM) or S2765 (1.2-1200 μM) and initiated with 5 nM of the FXa variants. The chromogenic conversion was assayed in the absence or presence of the direct FXa inhibitors apixaban, rivaroxaban, or edoxaban (0.0001-100 μM; SpecXa 250 μM) in order to determine IC_{50} concentrations for each free FXa variant.

2.9 | Inhibition of FXa by antithrombin

The rate of inactivation of FXa by AT was measured in assay buffer under pseudo-first-order rate conditions at ambient temperatures. Uncatalyzed reactions were prepared in assay buffer containing 0.1 to 0.8 μM AT and 7.5 nM FXa. At 0 to 110 minutes, residual enzyme activity was determined with the addition of 250 μM SpecXa. Reactions in the presence of UFH were prepared in assay buffer containing 0.5 to 6 mIE/mL UFH, 0.5 μM AT and initiated with 5 nM FXa. At 0.5 to 10 minutes, residual enzyme activity was determined with the addition of 250 μM SpecXa. The rate of AT inhibition was determined by fitting the obtained values to an exponential decay function ($k1$) and subsequent analysis by linear regression ($k2$) using GraphPad Prism software suite (GraphPad Software).

2.10 | Calibrated automated thrombography

Thrombin generation curves were obtained by supplementing normal pooled plasma with TF (2 or 6 pM), corn trypsin inhibitor (70 μg/mL),

PCPS (20 μM), and 15 to 45 μg/mL FX variant in the absence or presence of the direct FXa inhibitors apixaban, rivaroxaban, or edoxaban. Thrombin formation was initiated by addition of substrate buffer (FluCa), calcium, and the fluorogenic substrate (Z-Gly-Gly-Arg-AMC) to the plasma. The final reaction volume was 120 μL, of which 80 μL was plasma. Thrombin formation was determined every 15 seconds for 30 to 60 minutes and corrected for the calibrator using Thrombinoscope software (Thrombinoscope BV). The lag time, mean endogenous thrombin potential (ETP), thrombin peak height, and velocity index were calculated from at least 3 individual experiments performed in duplicate.

2.11 | MD simulations

MD simulations were performed using Amber2020 [42,43], starting from the 3-dimensional structure of the FXa-apixaban complex (Protein Data Bank [PDB] ID: 2P16). The protein, apixaban, and solvent (water) topologies were generated using tLeAP [43], as described in Supplementary Table S4. Following 2 energy minimization steps, 2 equilibration MD simulations were run at constant temperature and volume (NVT) and at constant pressure and temperature (NPT) equilibration steps, respectively. Subsequently, the production MD simulation extended over 1 μs (of which the first 2 ns were discarded for additional equilibration) with coordinates written out to disk every 0.2 ns. Detailed simulation settings and Amber input files for MD can be found in Supplementary Table S5. The PDB preparation setup for each MD step is described in the Supplementary Materials and Methods.

During post-MD data analysis, root-mean-square SD analysis was performed using AmberTools cpptraj [44]. The Gibbs free energy of apixaban binding (ΔGbind) was computed using a single-trajectory molecular mechanics Poisson–Boltzmann surface area (MM/PBSA) approach [45]. Prior to MM/PBSA binding free energy calculations, the topology of FXa and apixaban was extracted from the complex topology file using an ante-MMPBSA.py script in AmberTools with default Bondi radii settings [46]. The binding free energy of apixaban for FXa variants was calculated using the MMPBSA.py script in AmberTools [46] using default settings with an ionic strength set to 0.15 mM.

2.12 | Statistical analysis

All statistical analyses were computed using GraphPad Prism software. Kinetic data were analyzed by nonlinear regression using a 3-parameter logistic function. Parameters of calibrated automated thrombography in patient plasma and in the absence vs presence of TFPI-inhibiting antibodies were compared by 1-way analysis of variance. Statistical significance was accepted for a P value of $<.05$. All data are presented as mean ± 1 SD and are the result of at least 2 to 3 experiments unless stated otherwise.

3 | RESULTS

3.1 | Characterization of F174-substituted FX variants

In addition to the previously reported alanine replacement of the hydrophobic S4 subsite F174 in a partially purified FXa variant [35], here F174 was also substituted by a hydrophobic isoleucine or a hydrophilic serine residue, thereby generating FX-F174I and FX-F174S, respectively. Following stable FX expression in HEK293 cells, initial analysis of partially purified FXa variants using chromogenic substrate hydrolysis to evaluate FXa inhibition revealed a reduced apixaban inhibition (8- to 13-fold increased IC_{50} relative to wild-type r-FXa; Supplementary Figure S2), consistent with previous reports [35]. Given that all F174-substituted variants displayed similar IC_{50} values for apixaban inhibition, we next subjected FX-F174A and FX-F174S, in which F174 was replaced by an amino acid with substantially different properties in terms of side-chain dimensions or charge/hydrophobicity, respectively, to further characterization following purification. Sodium dodecyl sulfate–polyacrylamide gel electrophoresis analysis showed each FX(a) variant to migrate similar to wild-type r-FX(a) (Figure 1A, B, Supplementary Figure S3) [47]. Analysis of PT- or APTT-based fibrin clot formation initiated by the extrinsic (Figure 1C) or intrinsic (Figure 1D) coagulation pathway revealed FX-specific clotting activities in the same order of magnitude as those of r-FX, indicating that substitution of F174 by either alanine or serine does not severely impact FXa procoagulant function.

3.2 | F174 substitution in FX reduces the sensitivity for the direct FXa inhibitors

In concordance with a reduced apixaban inhibition in partially purified FXa variants (Supplementary Figure S2), assessing FXa inhibition by the direct FXa inhibitors through evaluation of chromogenic substrate hydrolysis in a purified system demonstrated a 2- to 5-fold reduced sensitivity for purified free FXa-F174 variants relative to r-FXa (Table 1). Assembly of FXa-F174 variants into prothrombinase resulted in a 5- to 10-fold decreased sensitivity for inhibition by either apixaban or edoxaban compared with r-FXa (Table 1). These results confirm our initial observations and suggest that F174-substituted FXa variants support thrombin generation in the presence of the direct FXa inhibitors.

To determine the capacity of the purified F174-substituted FX variants to overcome inhibition by the direct FXa inhibitors in a plasma system, their thrombin-forming potential was assessed using calibrated automated thrombography with a 6 pM TF-trigger resulting in direct FX activation by TF-FVIIa. Similar dose-response curves were obtained when determining the thrombin peak with increasing concentrations of FXa inhibitor in normal pooled plasma vs supplementation with r-FX at 3-fold the FX plasma concentration (30 μg/mL) [48] (Figure 2, Supplementary Table S1) [49]. With r-FX added, apixaban

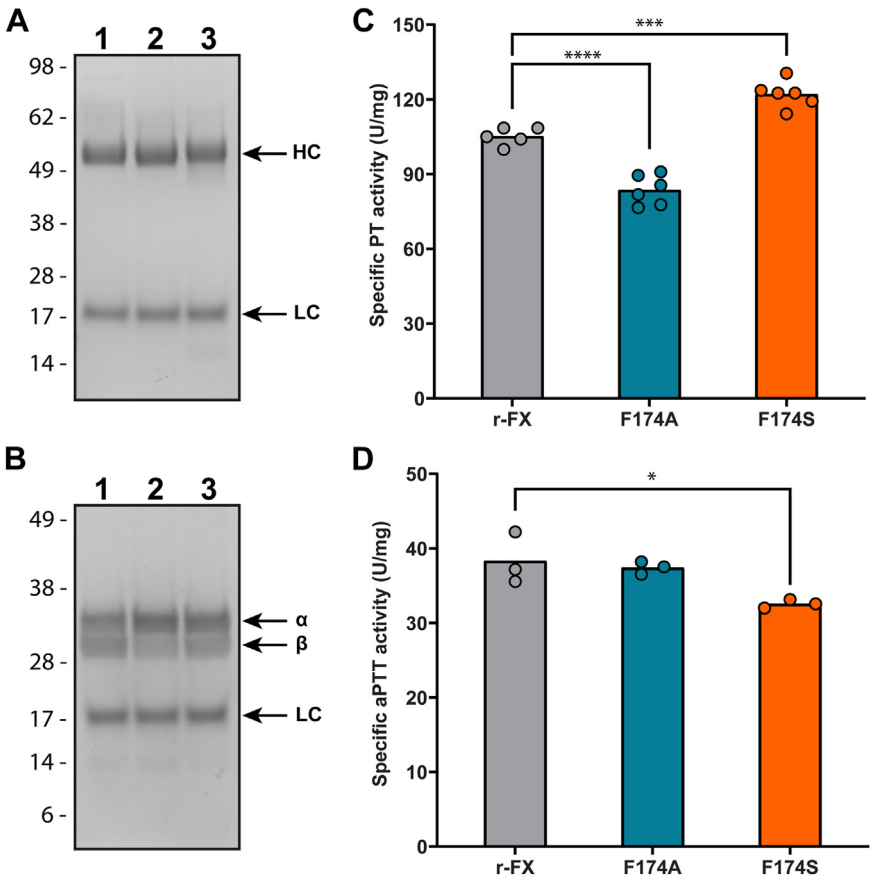

FIGURE 1 Characterization of F174-substituted factor (F)X(a) variants. (A–B) Sodium dodecyl sulfate–polyacrylamide gel electrophoresis (SDS-PAGE) analysis of purified recombinant FX (r-FX; A) or FXa (B) variants (2 μg/lane) under reducing conditions and visualized by staining with Coomassie Brilliant Blue R-250. Lane 1, wild-type FX(a); lane 2, FX(a)-F174A; lane 3, FX(a)-F174S. The protein bands corresponding to the FX heavy chain (HC), the heavy chain derived from α or β FXa (α or β), the FX(a) light chain (LC), and the apparent molecular weights (kDa) of the standards are indicated. The purified FXa products migrate as a mixture of α and β FXa, with the latter resulting from autoproteolytic excision of the C-terminal portion (residues 436-447) of FXa-α. Both α and β FXa isoforms are functionally similar with respect to prothrombinase assembly, prothrombin activation, antithrombin recognition, and peptidyl substrate conversion [47]. (C–D) The specific clotting activity of wild-type FX (r-FX), FX-F174A (F174A), or FX-F174S (F174S) initiated by the extrinsic (C) or intrinsic (D) pathway using a prothrombin time (PT)-based or activated partial thromboplastin time (APTT)-based assay as described in Materials and Methods. Briefly, FX variants were added to platelet-poor FX-depleted plasma, and coagulation was initiated using PT- or APTT-specific reagents. The coagulation time was monitored, and the specific activity was determined using reference curves of normal pooled plasma, assuming 1 U/mL FX equals 9 μg/mL FX. Mean values are given ± 1 SD. Data are representative of 3 independent experiments. $^{*}P < .05$; $^{***}P < .001$; $^{****}P < .0001$ according to 1-way analysis of variance.

dose-dependently decreased the thrombin peak with half-maximum inhibition at 0.14 μM apixaban (Figure 2A, Supplementary Table S1). The latter was markedly higher than the half-maximum values of free FXa inhibition in a purified system (Table 1) [3], which may be due to the plasma setting and supraphysiologic amounts of FX in this system. Conversely, supplementation of normal pooled plasma with FX-F174A or FX-F174S demonstrated a 15- to 30-fold reduction in apixaban sensitivity relative to r-FX (Figure 2A, Supplementary Table S1). Similarly, the F174-substituted FX variants demonstrated a 10- to 15-fold reduced sensitivity to inhibition by rivaroxaban or edoxaban compared with r-FX (Figure 2B, C, Supplementary Table S1). Next, the ability of the FX variants to support thrombin generation was explored under conditions when FX activation is mainly driven by FIXa [50,51] via the so-called "Josso loop" using a low amount of TF (2 pM). Similar to previous observations, supplementation with either FX-F174A or FX-F174S demonstrated a 10- to 40-fold reduced sensitivity for apixaban, rivaroxaban, or edoxaban relative to r-FX (Supplementary Figure S4 and Supplementary Table S1).

3.3 | F174-substituted FX variants bypass the direct FXa inhibitors and restore thrombin generation

To establish clinical relevance, we assessed whether the reduced sensitivity for the direct FXa inhibitors allowed FX-F174A and FX-F174S to overcome therapeutic peak inhibitor levels [52–54] using calibrated automated thrombography in response to a TF-trigger (6 pM). Following supplementation of normal pooled plasma with

TABLE 1 Inhibition and kinetic constants for free or prothrombinase-assembled factor Xa.

Factor Xa variants	Apixaban[a] IC_{50} (nM)	Rivaroxaban[a] IC_{50} (nM)	Edoxaban[a] IC_{50} (nM)	Apixaban[b] IC_{50} (nM)	Rivaroxaban[b] IC_{50} (nM)	Edoxaban[b] IC_{50} (nM)	Antithrombin[a] *k2*, uncatalyzed (M^{-1} S^{-1} × 10^3)	Antithrombin[a] *k2*, UFH (M^{-1} S^{-1} × 10^6)	TFPI[b] K_I (nM)
r-FXa	5.9 ± 0.3	2.5 ± 0.1	7.9 ± 0.2	9.2 ± 1.0	1.6 ± 0.2	5.3 ± 0.6	5.3 ± 0.1	2.0 ± 0.2	0.8 ± 0.04
FXa-F174A	20.9 ± 1.1[c]	14.3 ± 0.2[e]	28.5 ± 0.4[f]	57.5 ± 7.4[c]	12.1 ± 1.9	40.6 ± 4.3[d]	4.7 ± 0.5	2.6 ± 0.1	1.3 ± 0.25
FXa-F174S	24.6 ± 1.5[c]	9.6 ± 0.3[d]	16.5 ± 0.4[e]	55.6 ± 5.4[c]	16.2 ± 1.7	24.2 ± 2.6[c]	5.0 ± 0.5	3.8 ± 0.2	3.3 ± 0.48[c]

FX, factor FX; IC_{50}, half maximal inhibitory concentration; K_I, inhibitory constant; *k2*, rate constant of FXa-antithrombin formation; r-FX, recombinant FX; TFPI, tissue factor pathway inhibitor; UFH, unfractionated heparin.

[a] The constants for free FXa were obtained as described in Materials and Methods. Fitted values ± 1 SD of the induced fit are the means of 2 to 3 independent experiments.

[b] The constants for prothrombinase-assembled FXa were obtained as described in Materials and Methods. Fitted values ± 1 SD of the induced fit are the means of 2 to 3 independent experiments.

[c] $P < .05$ according to 1-way analysis of variance in comparison with r-FXa.

[d] $P < .01$ according to 1-way analysis of variance in comparison with r-FXa.

[e] $P < .001$ according to 1-way analysis of variance in comparison with r-FXa.

[f] $P < .0001$ according to 1-way analysis of variance in comparison with r-FXa.

apixaban, rivaroxaban, or edoxaban (1 μM), r-FX (60 μg/mL) only minimally improved the thrombin generation (up to 20% of normal pooled plasma peak height; Figure 3A). In contrast, supplementation of apixaban-treated normal pooled plasma with 30 μg/mL FX-F174A or FX-F174S fully restored the thrombin generation in the presence of apixaban, whereas 15 μg/mL improved the thrombin peak height to 75% of nontreated normal pooled plasma (Figure 3B). Similarly, the anticoagulant activity of rivaroxaban was completely reversed by the FX-F174 variants (Figure 3C) and improved up to 60% to 75% of normal pooled plasma in edoxaban-treated plasma (Figure 3D). This is consistent with the initially observed 11-fold increase in IC_{50} for edoxaban compared with the 15- to 35-fold increase for apixaban or rivaroxaban (Supplementary Table S1). Of note, supplementation with the FX-F174 variants prolonged both the lag time and time to peak up to 2-fold in the presence (Figure 3) but not in the absence of an inhibitor (Supplementary Figure S5). This delay in thrombin generation was not induced by a diminished FX activation, as activation by the intrinsic or extrinsic tenase complexes was unperturbed (Supplementary Table S2). Furthermore, no delay in the activation of FV was observed since FXa-F174A activated FV in an identical manner to r-FXa (Supplementary Figure S6). Assessment of the thrombin-forming potential under conditions of a limited TF-trigger (2 pM) revealed that the anticoagulant activity of the direct FXa inhibitors was largely reversed via supplementation with FX-F174A or FX-F174S (15-30 μg/mL; Supplementary Figure S7). Consistent with the results in the presence of a high TF-trigger (6 pM), the FX-F174 variants maintained an increased lag time relative to normal pooled plasma in the absence of an inhibitor.

3.4 | MD simulations show a decrease in affinity of apixaban binding to FX-F174A and FX-F174S

We performed MD simulations of the FXa variants to characterize the mechanisms of their reduced sensitivity to the FXa inhibitors. As a model for the latter, the interaction with apixaban, one of the more commonly used FXa inhibitors [55], was studied. The substitutions F174A, F174S, and F174F (wild-type control) were modeled into apixaban-bound FXa (PDB ID 2P16) [3], upon which 3 independent 1 μs MD simulation trajectories of the FXa-apixaban complexes were propagated. Calculation of the free energy of binding (ΔG_{bind}) to FXa using the MM/PBSA approach [45] indicated diminished binding of apixaban to FXa-F174A and FXa-F174S. Specifically, the average ΔG_{bind} for FXa-F174A and FXa-F174S was elevated (−2.3 ± 0.1 and −2.5 ± 0.1 kcal mol^{-1}, respectively) compared with wild-type FXa (−3.7 ± 0.1 kcal mol^{-1}; Figure 4) [56]. While being an approximation given the empirical nature of this approach, a 1.2 to 1.4 kcal mol^{-1} increase in ΔG_{bind} would be predictive of a 10-fold decrease in affinity. A residue-based analysis of apixaban-binding site interactions indicated a significantly reduced contribution to apixaban binding of residue 174 following substitution to Ala or Ser (Supplementary Figure S8). While this may be compensated to some extent by an increased contribution to ΔG_{bind} of Trp215 in FXa-F174A

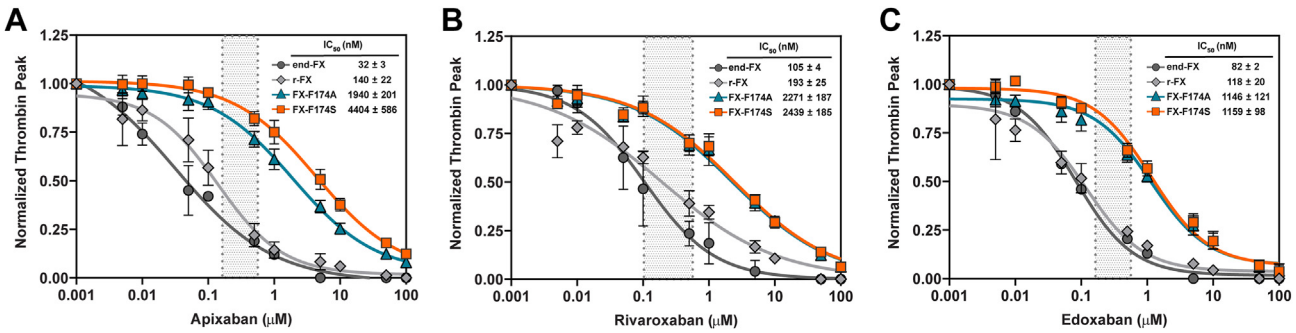

FIGURE 2 F174-substituted factor (F)X variants facilitate thrombin generation in the presence of direct FXa inhibitors. Thrombin generation was measured for 60 minutes at 37 °C in normal pooled plasma either without FX supplementation (endogenous FX only; end-FX, dark grey circles) or supplemented with 30 μg/mL of recombinant FX (r-FX; light grey diamonds), FX-F174A (blue triangles), or FX-F174S (orange squares) and increasing concentrations (1 nM to 100 μM) of apixaban (A), rivaroxaban (B), or edoxaban (C). Thrombin formation was triggered by the addition of 6 pM tissue factor in the presence of 20 μM small unilamellar phospholipid vesicles and initiated with $CaCl_2$ and a thrombin fluorogenic substrate as detailed in Materials and Methods. The thrombin peak height was normalized to the peak height in the absence of an inhibitor, and the lines were drawn by fitting the data to a 3-parameter logistic function upon which the half maximal inhibitory concentration (IC_{50}) ± 1 SD of the induced fits was obtained (Supplementary Table S1), which are shown in the insert. The grey dotted areas represent therapeutic peak inhibitor levels (apixaban, 0.15-0.55 μM; rivaroxaban, 0.10-0.57 μM; edoxaban, 0.16-0.43 μM) [49]. Data are representative of 3 independent experiments.

(Supplementary Figure S8), the diminished interaction with residue 174 observed in our MD simulations offers an explanation for the reduced inhibitor sensitivity when replacing F174. Interestingly, in the trajectory of the FXa wild-type model that featured a weaker ΔG_{bind} (−2.0 ± 0.1 kcal mol^{-1}; replicate 3), we observed partial dissociation of apixaban. This dissociation is reflected by the increase in root-mean-square displacement of apixaban during the simulation (Supplementary Figure S9). Notably, the partial dissociation of apixaban was accompanied by a loss in contact between its lactam moiety and FXa residue F174 (Supplementary Figure S10), further highlighting the relevance of F174 in inhibitor association.

3.5 | Reduced TFPI inhibition of F174-substituted FXa augments the direct FXa inhibitor bypassing effect

We next assessed the kinetic parameters of the FXa-F174 variants to examine the effects of F174 substitution on the FXa active site. Evaluation of the ability of the FXa variants to hydrolyze the FXa-specific chromogenic substrates SpecXa and S2765 revealed an altered k_{cat} of FXa-F174S relative to r-FXa (Table 2). Conversely, the binding affinities for the substrates were significantly altered in both FXa-F174 variants, indicative of a modified substrate binding cleft. This suggests that chromogenic substrates either engage the FXa S4 subsite [57] or F174 substitution induces conformational changes in the substrate binding region. Importantly, the kinetic parameters of prothrombin conversion by the FXa-F174 variants, as well as the apparent binding affinity for the FVa-like cofactor FV-810, were similar to those of r-FXa (Table 2). This demonstrates that the F174 modification does not significantly impact the assembly of the prothrombinase complex or the catalytic efficiency toward FXa's natural substrate prothrombin.

To examine the effects of F174 substitution on FXa inhibition, we assessed the second-order rate constants of the natural active site inhibitor AT. Inhibition of FXa-F174 variants proceeded at an identical rate relative to r-FXa in the absence or presence of UFH (Table 1), consistent with previous reports [35,58,59]. These observations might reflect the interaction of AT with the FXa S1 subsite rather than the S4 subsite, as shown by X-ray structures [60,61]. Interestingly, assessment of prothrombinase-assembled FXa inhibition by the natural active site inhibitor TFPI in a purified system revealed that FXa-F174S displayed a significant 4.5-fold reduced TFPI sensitivity relative to r-FXa, whereas no significant difference was observed for FXa-F174A (Figure 5, Table 1). These assessments were conducted employing FV-810 to assemble the prothrombinase complex. Given that FV-810 encompasses the acidic region (1493-1537) capable of binding to the basic region in the C-terminal domain of TFPI, these assays integrate the impact of TFPI binding to FV-810 [62]. To gain more insight into the TFPI resistance, we next explored the thrombin-forming potential of FX-F174 variants using calibrated automated thrombography in FX-depleted plasma supplemented with 10 μg/mL FX variant and monoclonal antibodies that specifically block the function of individual TFPI domains. In the absence of TFPI antibodies, FX-F174 variants displayed a 2-fold increase in thrombin peak relative to r-FX (Supplementary Figure S11). In contrast, similar thrombin peaks were observed for all FX variants with TFPI-inhibiting antibodies. This indicates that the heightened thrombin-forming potential of FX-F174A and FX-F174S is induced by a partial loss of TFPI inhibition. As such, these results suggest an additional mode of action by which the F174-substituted FX variants bypass the direct FXa inhibitors.

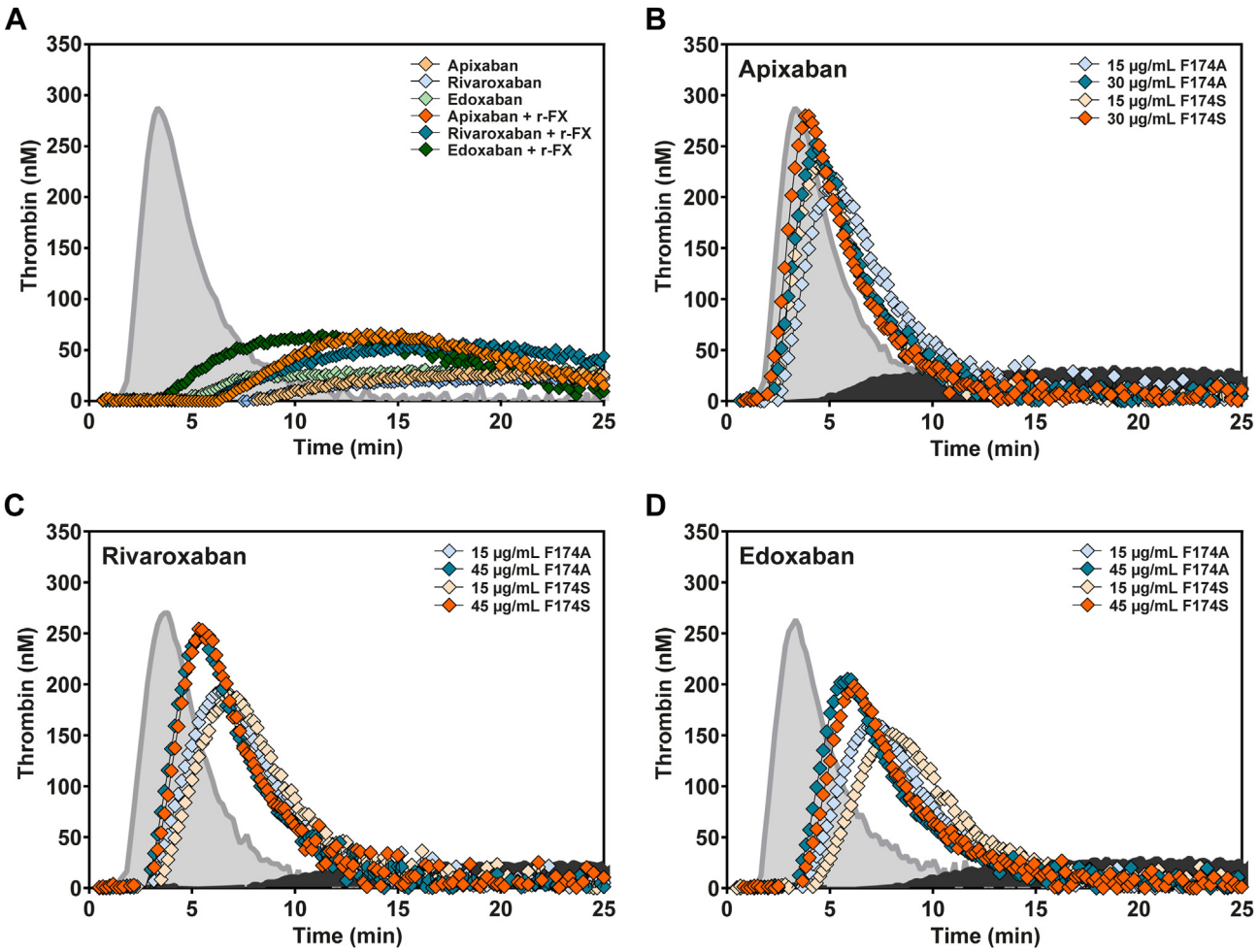

FIGURE 3 F174-substituted factor (F)X variants restore thrombin generation in inhibitor-spiked plasma. Thrombin generation was measured for 60 minutes at 37 °C in normal pooled plasma supplemented with (A) 1 µM apixaban, rivaroxaban, or edoxaban in the absence (*yellow, light blue, or light green diamonds, respectively*) or with the addition of 60 µg/mL recombinant FX (r-FX; *orange, dark blue, or dark green, respectively*), (B) 1 µM apixaban with the addition of 15 to 30 µg/mL FX-F174A (*light blue-dark blue diamonds*) or 15 to 30 µg/mL FX-F174S (*yellow-orange diamonds*), or (C) 1 µM rivaroxaban with the addition of 15 to 45 µg/mL FX-F174A (*light blue-dark blue diamonds*) or 15 to 45 µg/mL FX-F174S (*yellow-orange diamonds*), or (D) 1 µM edoxaban with the addition of 15 to 45 µg/mL FX-F174A (*light blue-dark blue diamonds*) or 15 to 45 µg/mL FX-F174S (*yellow-orange diamonds*). Thrombin formation was triggered by the addition of 6 pM tissue factor in the presence of 20 µM small unilamellar phospholipid vesicles and initiated with $CaCl_2$ and a thrombin fluorogenic substrate as detailed in Materials and Methods. The thrombin generation curves of normal pooled plasma in the absence (A–D; light grey area under the curve) or presence (B–D; dark grey area under the curve) of the inhibitors are shown. Data sets are representatives of 3 independent experiments.

3.6 | F174-substituted FX reverses the anticoagulant activity of apixaban and rivaroxaban in atrial fibrillation and venous thromboembolism patient plasma

The ability of the FX-F174 variants to bypass the direct FXa inhibitors was validated in plasma derived from nonvalvular atrial fibrillation or venous thromboembolic disease patients who were treated with apixaban or rivaroxaban (Supplementary Table S3) using calibrated automated thrombography in response to a high TF-trigger (6 pM). As FX-F174A and FX-F174S displayed similar activities in previous experiments, we selected FX-F174A for assessment in patient plasma. Assessment of the thrombin-forming potential demonstrated that supplementation of patient plasma with FX-F174A increased the thrombin peak in all individual patient samples (Figure 6A, B, Supplementary Figure S12). In atrial fibrillation patient plasma, the thrombin peak increased to near-normal pooled plasma conditions (290-330 nM). While plasma from patients with atrial fibrillation or venous thromboembolic disease displayed a prolonged lag time relative to normal pooled plasma (Figure 6C), this was markedly shortened by supplementation with FX-F174A in all individual patient samples (Figure 6C, D). Additional assessment revealed that FX-F174A reversed the anticoagulant effect on the thrombin generation velocity in a similar manner as described for the thrombin peak and lag time (Supplementary Figure S13A, B). In contrast, the ETP in atrial fibrillation and venous thromboembolic disease patient plasma was modestly reduced in the absence of FX-F174A relative to normal pooled plasma (Supplementary Figure S13C, D) as a result of the

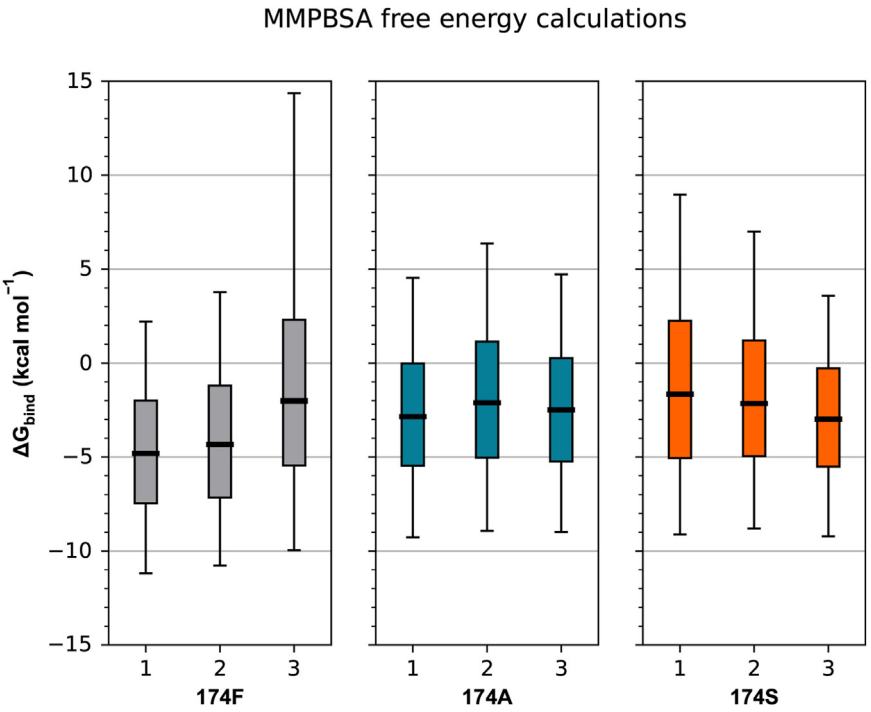

FIGURE 4 Calculated free energy of apixaban binding to factor (F)Xa variants. Molecular mechanics Poisson–Boltzmann surface area (MM/PBSA) binding free energies (ΔG_{bind}) of apixaban binding to wild-type FXa (174F), FXa-F174A (174A), or FXa-F174S (174S) were calculated for each independent 1 μs molecular dynamics simulation with 3 replicates shown per FXa species. The data are presented as boxplots, with the whiskers representing the 5th to 95th percentile of the data set. Statistical significance: $^{*}P < .05$; $^{****}P < .0001$. Data were visualized using Matplotlib [56]. Molecular configurations at 250, 500, 705, and 900 ns of each simulation are shown in Supplementary Figures S10, S14, and S15.

inhibitor-induced extension of the thrombin generation curves over time. Despite this, FX-F174A supplementation elevated the ETP in all patient groups, demonstrating that F174-substituted FX variants have the ability to reverse the anticoagulant activity of the direct FXa inhibitors in patient plasma.

4 | DISCUSSION

In this study, we present FX variants that could act as prohemostatic bypassing agents by supporting coagulation in the presence of direct FXa inhibitors. We showed that the FX variant FX-F174A comprising a single substitution in the S4 subsite effectively counteracted the anticoagulant effects of apixaban or rivaroxaban in plasma from nonvalvular atrial fibrillation and venous thromboembolic patients. While FX-F174A is inhibited by rivaroxaban and apixaban to some extent, FX-F174A is nonetheless capable of promoting thrombin formation in the presence of therapeutic concentrations of FXa inhibitors. Unfortunately, we were unable to obtain plasma samples from the same individual patients before treatment initiation. As thrombin generation profiles of individual plasmas can vary substantially, such samples would provide valuable information on the level of anticoagulant reversal in these patients [63]. Nevertheless, FX-F174A successfully restored the thrombin-forming potential within the therapeutically useful inhibitor range (>100 nM), at which patients are likely at an increased risk of bleeding [54].

TABLE 2 Kinetic parameters for peptidyl substrate and macromolecular substrate conversion.

Factor Xa variants	SpecXa[a] K_m (μM)	SpecXa[a] k_{cat} (min^{-1})	S2765[a] K_m (μM)	S2765[a] k_{cat} (min^{-1})	Prothrombin[b] K_m (μM)	Prothrombin[b] k_{cat} (min^{-1})	Cofactor Va[b] $K_{d,\ app}$ (nM)
r-FXa	113 ± 9	23.9 ± 0.6	85 ± 10	34.3 ± 1.1	0.52 ± 0.10	960 ± 83	0.8 ± 0.2
FXa-F174A	251 ± 7[d]	25.8 ± 0.3	360 ± 33[c]	32.6 ± 1.2	0.70 ± 0.23	1041 ± 163	1.2 ± 0.1[c]
FXa-F174S	186 ± 9[c]	30.6 ± 0.6[d]	217 ± 17[d]	21.9 ± 0.6[e]	0.69 ± 0.08	1152 ± 73	0.9 ± 0.2

FX, factor FX; k_{cat}, turnover number of enzyme; $K_{d,\ app}$, apparent dissociation constant; K_m, michaelis constant; r-FX, recombinant FX; SpecXa, peptidyl substrate methoxycarbonylcyclohexyl-Gly-Gly-Arg-pNA.

[a] The kinetic constants for free FXa were obtained as described in Materials and Methods. Fitted values ± 1 SD of the induced fit are the means of 2 to 3 independent experiments.

[b] The kinetic constants for prothrombinase-assembled FXa were obtained as described in Materials and Methods. Fitted values ± 1 SD of the induced fit are the means of 2 to 3 independent experiments.

[c] $P < .05$ according to 1-way analysis of variance in comparison with r-FXa.

[d] $P < .01$ according to 1-way analysis of variance in comparison with r-FXa.

[e] $P < .0001$ according to 1-way analysis of variance analysis in comparison with r-FXa.

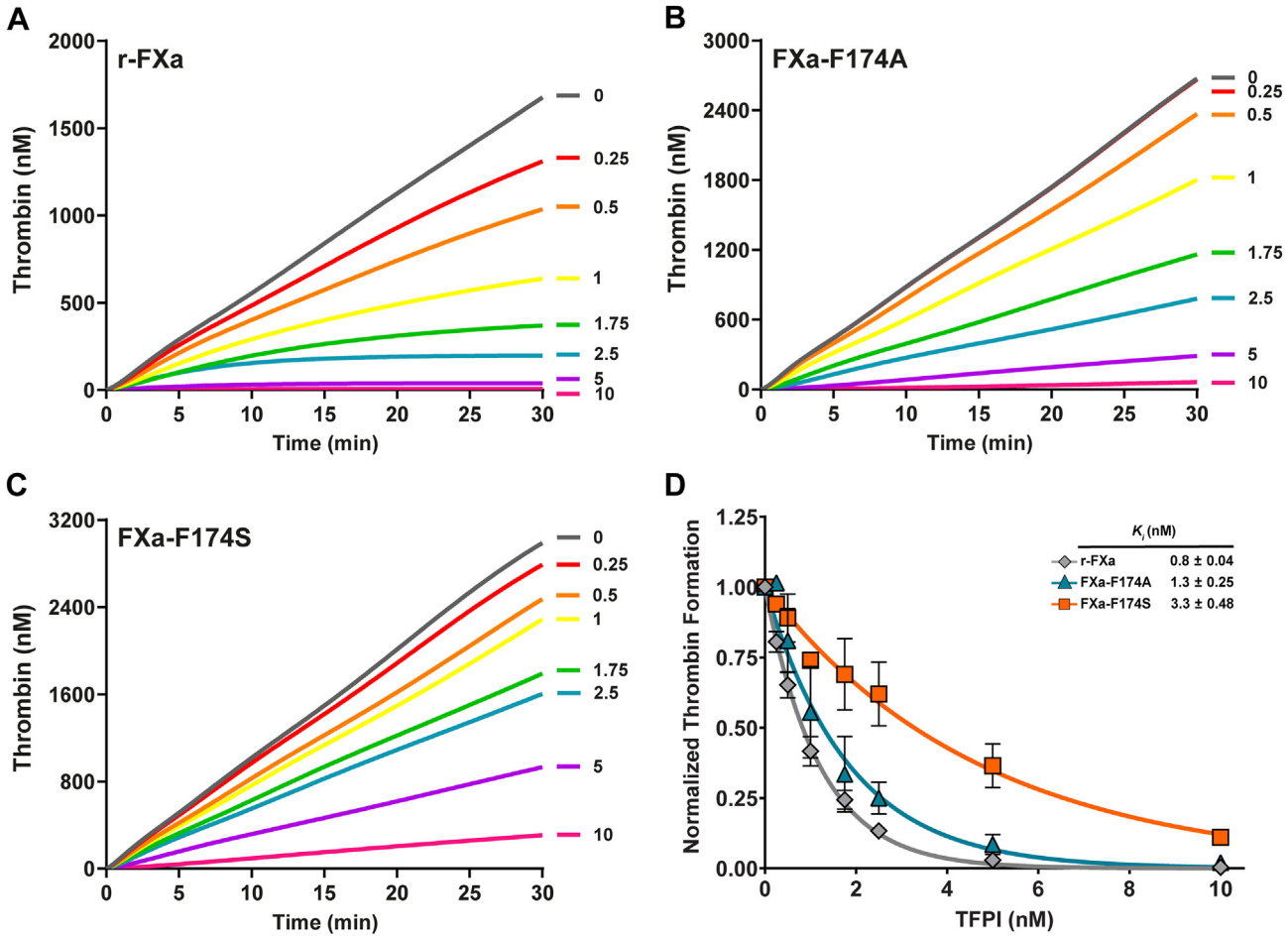

FIGURE 5 Inhibition of factor (F)Xa variants by tissue factor pathway inhibitor (TFPI). The inhibition of FXa by TFPI was assessed by measuring the prothrombinase-dependent conversion of prothrombin. Reaction mixtures containing 1.4 μM prothrombin, 2 nM FV-810, 50 μM small unilamellar phospholipid vesicles, and 10 μM dansylarginine-N-(3-ethyl-1,5-pentanediyl)amide were initiated with 0.05 nM recombinant FXa (r-FXa; A), FXa-F174A (B), or FXa-F174S (C) in the presence of 0 to 10 nM TFPIα (r-TFPI, Tifacogin, Novartis). At selected time intervals, samples were removed, and thrombin formation was assessed by S2238 (250 μM) conversion. The data were corrected for substrate consumption as described in Materials and Methods. The data sets are representative of 2 independent experiments. (D) Thrombin formed at 30 minutes in the presence of TFPI was normalized to the value obtained in the absence of an inhibitor. The lines were drawn after fitting all datasets to a 1-phase decay equation, and the fitted inhibition constants are shown in the inset. Mean values ± 1 SD of 2 independent experiments are provided.

In the presence of therapeutic peak concentrations of FXa inhibitor, we were able to restore thrombin generation by supplementation with purified FX-F174A or FX-F17S (15-45 μg/mL), requiring a 1.5- to 4.5-fold higher plasma level of FX-F174 variant relative to endogenous FX (~10 μg/mL) [64] to bypass the direct FXa inhibitors. We propose that these required concentrations arise from competition for FX activation by the intrinsic and extrinsic tenase coagulation complexes. The role of competitive activation is further supported by the similar kinetic constants for the intrinsic or extrinsic activation of FX and FX-F147 variants. Similarly, we observed identical kinetics for the activation of FV by either FXa-F174A or r-FXa. While it is possible that FV activation is delayed in the presence of the direct FXa inhibitors, which may explain the up to 2-fold prolonged lag time observed for FX-174 variants, we surmise that the direct FXa inhibitors are acting on the small quantities of FXa formed during the initial phase of coagulation. The differences in the affinity of these inhibitors for FXa may therefore induce the observed inhibitor-dependent prolongation in lag time in thrombin generation.

Interestingly, we observed a reduced sensitivity of FXa-F174 variants for the natural FXa inhibitor TFPI. Previous studies have shown that the inhibition or sequestration of TFPI could restore hemostasis in hemophilic plasma and patients [25,26,65–67], thus providing evidence for an additional mode of action by which the FX-F174 variants are able to bypass direct FXa inhibitors. Despite the 3-fold reduction in TFPI sensitivity of FXa-F174S relative to FXa-F174A, these minor functional differences may be explained by the relatively low plasma concentration of free TFPIα (~0.3 nM) [68,69]. The partial resistance for TFPI displayed by FX-F174A and FX-174S is concurrent to the elevated IC_{50} values of direct FXa inhibitors observed in plasma relative to the inhibition of free or prothrombinase-assembled FXa.

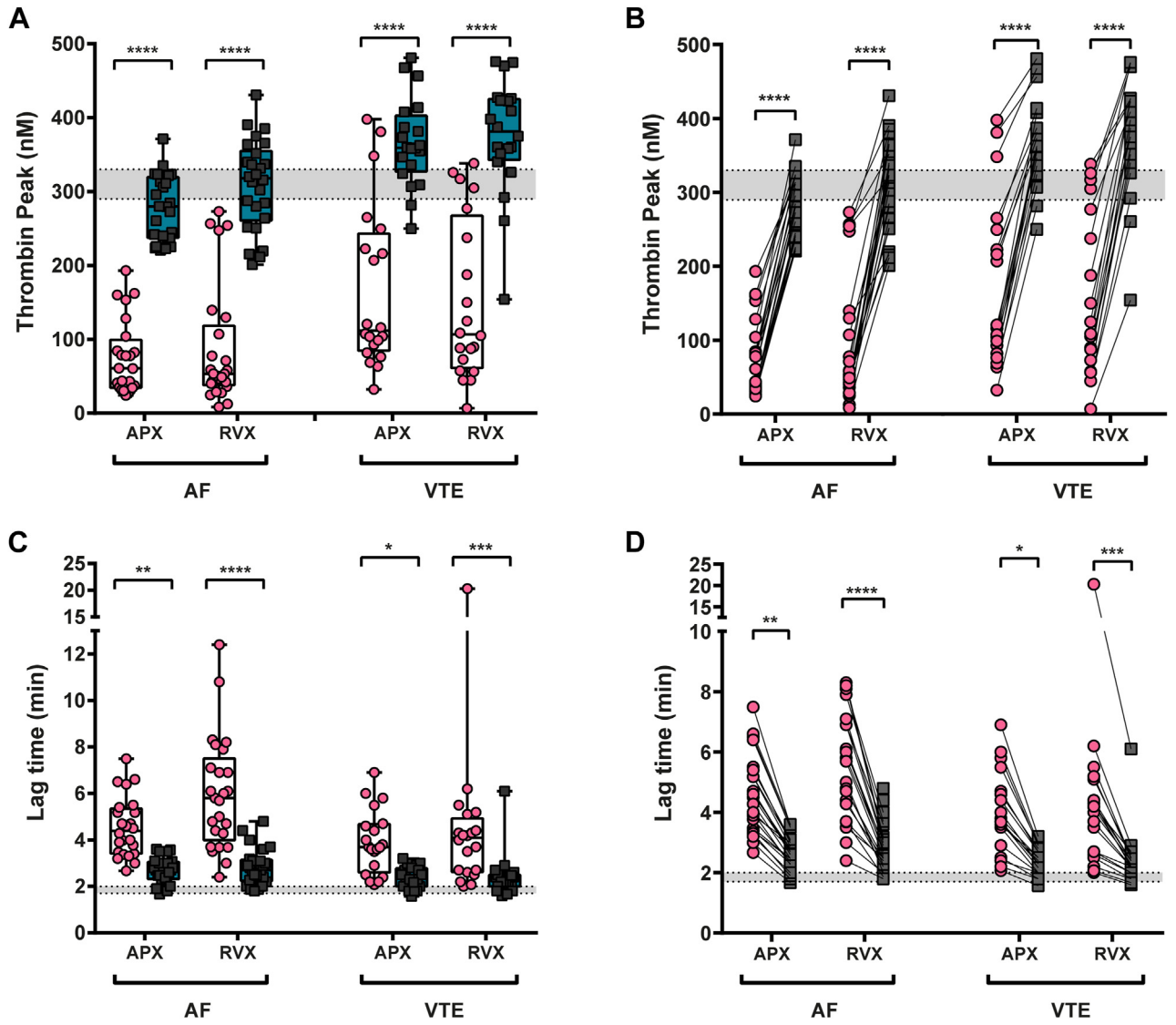

FIGURE 6 Reversal of the anticoagulant activity of apixaban (APX) or rivaroxaban (RVX) in atrial fibrillation (AF) and venous thromboembolism (VTE) patient plasma. Thrombin generation was measured for 60 minutes at 37 °C in plasma from AF or VTE patients treated with APX or RVX in the absence (*pink dots*) or supplemented with 30 μg/mL factor (F)X-F174A (*grey squares*). Thrombin formation was triggered by the addition of 6 pM tissue factor in the presence of 20 μM small unilamellar phospholipid vesicles and initiated with $CaCl_2$ and a thrombin fluorogenic substrate as detailed in Materials and Methods. Box plots of the thrombin peak (A) and lag time (C) are shown for the different patient groups, and in panels (B) and (D), the thrombin peak and lag time values in the absence or presence of FX-F174A are shown for the individual patients. Grey dotted areas represent normal pooled plasma values (n = 13; thrombin peak, 290-330 nM; lag time, 1.7-2 minutes). *P < .05; **P < .01; ***P < .001; ****P < .0001 according to 1-way analysis of variance. Each data point represents a measurement performed in duplicate for each patient sample.

Collectively, our findings reveal that FX-F174A and FX-F174S bypass direct FXa inhibitors via a unique mechanism compared with previously described reversal agents and indicate that modulation of FXa inhibition by TFPI is a promising strategy to overcome the anticoagulant effects of direct FXa inhibitors.

Previously, Qu et al. [70] used MD simulations to identify destabilized binding of rivaroxaban to similar FXa variants. In our setup, a destabilized inhibitor binding is an indication of the bypassing qualities of the variants. Following this idea, we employed longer MD simulations to investigate the bypassing qualities of FXa-F174A and FXa-F174S by comparing the free energy of apixaban association of these variants to a wild-type FXa model. Using the MM/PBSA approach, we found that diminished interaction between apixaban and the F174 residue led to a decrease in inhibitor binding affinity. Interestingly, in a single MD trajectory, we observed the partial dissociation of apixaban initiated by the displacement of the F174 residue that highlights the importance of this residue and suggests a further mechanistic role for later *in silico* investigation. Naturally, the diminished association of apixaban for the S4 subsites of FXa-F174A and FXa-F174S found in our MD simulations arises from the

reduced interaction of the smaller, nonaromatic 174 residues with the lactam moiety of apixaban. We surmise that the diminished association gives rise to the experimentally observed bypassing qualities of FX-F174A and FX-F174S for apixaban as well as other FXa inhibitors (ie, rivaroxaban and TFPI).

In addition to inhibitor bypassing activity, FXa-F174A and FXa-F174S exhibit reduced catalytic activity toward FXa-specific chromogenic substrates. As this effect is not seen in plasma clotting and kinetic assays, we infer that prothrombin does not engage in productive interactions with the S4 subsite of FXa. Interestingly, these results might suggest that exosites in FXa and prothrombin drive the proteolytic cleavage at the prothrombin activation residues R271 and R320 [71,72]. Although our data do not provide any indication, it should be noted that the FXa-F174 variants might have potential off-target interactions that have not been uncovered by the *in vitro* experimental systems.

Unfortunately, we were unable to assess the efficacy of FX-F174 variants *in vivo*. Preliminary data obtained using a mouse tail clip model indicated significant bleeding following administration of 10 mg/kg apixaban. In similar fashion, previous studies made use of 1 to 10 mg/kg direct FXa inhibitor for *in vivo* reversal experiments [28,33,73,74], equating to supraphysiological plasma concentrations of ~0.2 to 2 mM and representing a >1000-fold increase relative to peak inhibitor concentrations observed in patients [52–54]. While the FX-F174 variants effectively counteracted the anticoagulant effects at inhibitor concentrations of ≤1 μM, they would be completely inhibited using *in vivo* FXa inhibitor concentrations >1 μM. Furthermore, in contrast to antidote-based reversal agents, our FX-F174 variants rely on proteolytic activation by interacting with endogenous coagulation factors. Previously, we revealed significantly reduced calibrated automated thrombography parameters and higher anti-FXa activity in murine plasma relative to human plasma [75], pointing to striking differences between rodent and human plasma systems. In contrast to the human system, in mice, full-length TFPI does not circulate in plasma but is expressed at the endothelial surface and is present in platelets [76]. Furthermore, murine full-length TFPI exhibits an insertion in the basic region of the TFPI C-terminal domain [69], of which the effect on the interaction with FV remains to be determined. As such, preclinical assessment of prohemostatic agents in murine models may prove difficult to reliably extrapolate to a human system. As an alternative, we have validated the ability of FX-F174 variants to revert the anticoagulant effects in plasma samples of apixaban- and rivaroxaban-treated patients, providing valuable evidence for their potential as specific reversal agents.

A limitation of our approach may be the use of a recombinant protein variant that could elicit an immunogenic response, thereby limiting the efficacy of repeated use. Since our FX variants comprise a single amino acid substitution, the risk of immunogenicity might be minimal. Thus far, neutralizing antibody responses against andexanet alfa have not been reported, nor have antibodies with cross-reactivity to FX(a) been detected [17,77]. Nonneutralizing antibodies have been developed, albeit with generally low antibody titers [77]. Importantly, only a few cases of patients with acquired inhibitors against therapeutic FX have been reported in the setting of FX deficiency [78], suggesting that either FX (or its derived variants) have little immunogenic potential. It is also important to note that prohemostatic bypassing agents may significantly increase the risk of thrombotic complications and therefore require intensive evaluation in clinical practice. For safety purposes, here we have employed F174-substituted FX variants in an inactive zymogen form to prevent potential macromolecular interactions. Upon the initiation of secondary hemostasis, the FX-F174 variants are activated through the intrinsic and extrinsic pathways similar to endogenous FX. As such, major disturbances that could fail to stop bleeding or otherwise induce pathological thrombosis may be prevented.

In conclusion, our findings show that via a single residue substitution at F174, we have created FX variants that bypass direct FXa inhibitors while remaining partially sensitive to inhibition by TFPI. These results further highlight the role of the S4 subsite interactions for the direct inhibition of direct FXa inhibitors (ie, apixaban, rivaroxaban, and TFPI) [35]. Results from MM/PBSA binding free energy analyses revealed that FX-F174A and FX-F174S have a decreased affinity for apixaban, providing insight into the mechanism for direct inhibitor bypassing. The potential of FX-F174 variants was further established by reversing the anticoagulant activity of apixaban and rivaroxaban in plasma of atrial fibrillation and venous thromboembolic patients. As such, FX-F174A and FX-F174S variants have the potential to serve as a rapid-onset prohemostatic bypassing strategy to counteract life-threatening bleeding complications as a result of direct FXa inhibitors.

ACKNOWLEDGMENTS

This work was financially supported by the Landsteiner Foundation for Blood Transfusion (LSBR, grant number 1451) and the PPS Allowance Health~Holland, Top Sector Life Sciences & Health. The funding agencies had no role in the preparation, review, or approval of the manuscript.

AUTHOR CONTRIBUTIONS

Designed research: M.S., D.A.P. III, D.P.G., and M.H.A.B. Performed research: M.S., G.J., D. Veizaj, K.L.C., G.P., and D. Verhoef. Contribution of crucial new reagents/analytic tools: G.J., S.T., A.S., T.M.H., P.G., and V.S. Data analysis: M.S., D. Veizaj, D.A.P. III, K.L.C., D.P.G., P.H.R., and M.H.A.B. Writing – original draft: M.S. and D. Veizaj. Writing – review and editing: G.J., D. Veizaj., D.A.P. III, D. Verhoef, T.M.H., P.G., P.H.R., D.P.G., V.S., and M.H.A.B.

DECLARATION OF COMPETING INTERESTS

P.H.R. and D. Verhoef own equity in VarmX B.V. T.M.H. and S.T. own equity in Coagulation Profile B.V. M.H.A.B. has received consultancy fees from VarmX B.V. (all fees to the institution) and is inventor on intellectual property related to this work. The remaining authors declare no competing financial interests.

REFERENCES

[1] Wendelboe AM, Raskob GE. Global burden of thrombosis: epidemiologic aspects. *Circ Res*. 2016;118:1340–7.

[2] Roehrig S, Straub A, Pohlmann J, Lampe T, Pernerstorfer J, Schlemmer KH, Reinemer P, Perzborn E. Discovery of the novel antithrombotic agent 5-chloro-N-({(5S)-2-oxo-3- [4-(3-oxomorpholin-4-yl)phenyl]-1,3-oxazolidin-5-yl}methyl)thiophene- 2-carboxamide (BAY 59-7939): an oral, direct factor Xa inhibitor. *J Med Chem*. 2005;48:5900–8.

[3] Pinto DJ, Orwat MJ, Koch S, Rossi KA, Alexander RS, Smallwood A, Wong PC, Rendina AR, Luettgen JM, Knabb RM, He K, Xin B, Wexler RR, Lam PY. Discovery of 1-(4-methoxyphenyl)-7-oxo-6-(4-(2-oxopiperidin-1-yl)phenyl)-4,5,6,7-tetrahydro-1H -pyrazolo[3,4-c] pyridine-3-carboxamide (apixaban, BMS-562247), a highly potent, selective, efficacious, and orally bioavailable inhibitor of blood coagulation factor Xa. *J Med Chem*. 2007;50:5339–56.

[4] Furugohri T, Isobe K, Honda Y, Kamisato-Matsumoto C, Sugiyama N, Nagahara T, Morishima Y, Shibano T. DU-176b, a potent and orally active factor Xa inhibitor: in vitro and in vivo pharmacological profiles. *J Thromb Haemost*. 2008;6:1542–9.

[5] Zhang P, Huang W, Wang L, Bao L, Jia ZJ, Bauer SM, Goldman EA, Probst GD, Song Y, Su T, Fan J, Wu Y, Li W, Woolfrey J, Sinha U, Wong PW, Edwards ST, Arfsten AE, Clizbe LA, Kanter J, et al. Discovery of betrixaban (PRT054021), N-(5-chloropyridin-2-yl)-2-(4-(N, N-dimethylcarbamimidoyl)benzamido)-5-methoxybenz amide, a highly potent, selective, and orally efficacious factor Xa inhibitor. *Bioorg Med Chem Lett*. 2009;19:2179–85.

[6] Hauel NH, Nar H, Priepke H, Ries U, Stassen JM, Wienen W. Structure-based design of novel potent nonpeptide thrombin inhibitors. *J Med Chem*. 2002;45:1757–66.

[7] Weitz JI, Harenberg J. New developments in anticoagulants: past, present and future. *Thromb Haemost*. 2017;117:1283–8.

[8] Connolly SJ, Ezekowitz MD, Yusuf S, Eikelboom J, Oldgren J, Parekh A, Pogue J, Reilly PA, Themeles E, Varrone J, Wang S, Alings M, Xavier D, Zhu J, Diaz R, Lewis BS, Darius H, Diener HC, Joyner CD, Wallentin L, et al. Dabigatran versus warfarin in patients with atrial fibrillation. *N Engl J Med*. 2009;361:1139–51.

[9] Patel MR, Mahaffey KW, Garg J, Pan G, Singer DE, Hacke W, Breithardt G, Halperin JL, Hankey GJ, Piccini JP, Becker RC, Nessel CC, Paolini JF, Berkowitz SD, Fox KA, Califf RM, ROCKET AF Investigators. Rivaroxaban versus warfarin in nonvalvular atrial fibrillation. *N Engl J Med*. 2011;365:883–91.

[10] Agnelli G, Buller HR, Cohen A, Curto M, Gallus AS, Johnson M, Masiukiewicz U, Pak R, Thompson J, Raskob GE, Weitz JI, AMPLIFY Investigators. Oral apixaban for the treatment of acute venous thromboembolism. *N Engl J Med*. 2013;369:799–808.

[11] Deitelzweig SB, Johnson BH, Lin J, Schulman KL. Prevalence of clinical venous thromboembolism in the USA: current trends and future projections. *Am J Hematol*. 2011;86:217–20.

[12] Chugh SS, Havmoeller R, Narayanan K, Singh D, Rienstra M, Benjamin EJ, Gillum RF, Kim YH, McAnulty JH Jr, Zheng ZJ, Forouzanfar MH, Naghavi M, Mensah GA, Ezzati M, Murray CJ. Worldwide epidemiology of atrial fibrillation: a Global Burden of Disease 2010 Study. *Circulation*. 2014;129:837–47.

[13] Nazha B, Pandya B, Cohen J, Zhang M, Lopes RD, Garcia DA, Sherwood MW, Spyropoulos AC. Periprocedural outcomes of direct oral anticoagulants versus warfarin in nonvalvular atrial fibrillation. *Circulation*. 2018;138:1402–11.

[14] Sharma M, Cornelius VR, Patel JP, Davies JG, Molokhia M. Efficacy and harms of direct oral anticoagulants in the elderly for stroke prevention in atrial fibrillation and secondary prevention of venous thromboembolism: systematic review and meta-analysis. *Circulation*. 2015;132:194–204.

[15] Loo SY, Dell'Aniello S, Huiart L, Renoux C. Trends in the prescription of novel oral anticoagulants in UK primary care. *Br J Clin Pharmacol*. 2017;83:2096–106.

[16] Zhu J, Alexander GC, Nazarian S, Segal JB, Wu AW. Trends and variation in oral anticoagulant choice in patients with atrial fibrillation, 2010-2017. *Pharmacotherapy*. 2018;38:907–20.

[17] Connolly SJ, Crowther M, Eikelboom JW, Gibson CM, Curnutte JT, Lawrence JH, Yue P, Bronson MD, Lu G, Conley PB, Verhamme P, Schmidt J, Middeldorp S, Cohen AT, Beyer-Westendorf J, Albaladejo P, Lopez-Sendon J, Demchuk AM, Pallin DJ, Concha M, et al. Full study report of andexanet alfa for bleeding associated with factor Xa inhibitors. *N Engl J Med*. 2019;380:1326–35.

[18] Connolly S, Sharma M, Cohen AT, Demchuk AM, Czonkowska A, Lindgren AG, Molina CA, Bereczki D, Toni D, Seiffge DJ, Tanne D, Sandset EC, Tsivgoulis G, Christensen H, Beyer-Westendorf J, Coutinho JM, Crowther M, Verhamme P, Amarenco P, Roine RO, et al. Andexanet for factor Xa inhibitor-associated acute intracerebral hemorrhage. *N Engl J Med*. 2024;390:1745–55.

[19] Majeed A, Agren A, Holmstrom M, Bruzelius M, Chaireti R, Odeberg J, Hempel EL, Magnusson M, Frisk T, Schulman S. Management of rivaroxaban- or apixaban-associated major bleeding with prothrombin complex concentrates: a cohort study. *Blood*. 2017;130:1706–12.

[20] Schulman S, Gross PL, Ritchie B, Nahirniak S, Lin Y, Lieberman L, Carrier M, Crowther MA, Ghosh I, Lazo-Langner A, Zondag M, Study I. prothrombin complex concentrate for major bleeding on factor Xa inhibitors: a prospective cohort study. *Thromb Haemost*. 2018;118:842–51.

[21] Arachchillage DRJ, Alavian S, Griffin J, Gurung K, Szydlo R, Karawitage N, Laffan M. Efficacy and safety of prothrombin complex concentrate in patients treated with rivaroxaban or apixaban compared to warfarin presenting with major bleeding. *Br J Haematol*. 2019;184:808–16.

[22] Pollack CV Jr, Reilly PA, van Ryn J, Eikelboom JW, Glund S, Bernstein RA, Dubiel R, Huisman MV, Hylek EM, Kam CW, Kamphuisen PW, Kreuzer J, Levy JH, Royle G, Sellke FW, Stangier J, Steiner T, Verhamme P, Wang B, Young L, et al. Idarucizumab for dabigatran reversal - full cohort analysis. *N Engl J Med*. 2017;377:431–41.

[23] Goldstein JN, Refaai MA, Milling TJ Jr, Lewis B, Goldberg-Alberts R, Hug BA, Sarode R. Four-factor prothrombin complex concentrate versus plasma for rapid vitamin K antagonist reversal in patients needing urgent surgical or invasive interventions: a phase 3b, open-label, non-inferiority, randomised trial. *Lancet*. 2015;385:2077–87.

[24] Sarode R, Milling TJ Jr, Refaai MA, Mangione A, Schneider A, Durn BL, Goldstein JN. Efficacy and safety of a 4-factor prothrombin complex concentrate in patients on vitamin K antagonists presenting with major bleeding: a randomized, plasma-controlled, phase IIIb study. *Circulation*. 2013;128:1234–43.

[25] Ersayin A, Thomas A, Seyve L, Thielens N, Castellan M, Marlu R, Polack B, Dagher MC. Catalytically inactive Gla-domainless factor Xa binds to TFPI and restores ex vivo coagulation in hemophilia plasma. *Haematologica*. 2017;102:e483–5.

[26] Marlu R, Polack B. Gla-domainless factor Xa: molecular bait to bypass a blocked tenase complex. *Haematologica*. 2012;97:1165–72.

[27] Schreuder M, Reitsma PH, Bos MHA. Reversal agents for the direct factor Xa inhibitors: biochemical mechanisms of current and newly emerging therapies. *Semin Thromb Hemost*. 2020;46:986–98.

[28] Lu G, DeGuzman FR, Hollenbach SJ, Karbarz MJ, Abe K, Lee G, Luan P, Hutchaleelaha A, Inagaki M, Conley PB, Phillips DR, Sinha U. A specific antidote for reversal of anticoagulation by direct and indirect inhibitors of coagulation factor Xa. *Nat Med*. 2013;19:446–51.

[29] Schreuder M, Reitsma PH, Bos MHA. Blood coagulation factor Va's key interactive residues and regions for prothrombinase assembly and prothrombin binding. *J Thromb Haemost*. 2019;17:1229–39.

[30] Huntington JA, Read RJ, Carrell RW. Structure of a serpin-protease complex shows inhibition by deformation. *Nature*. 2000;407:923–6.

[31] Jourdi G, Gouin-Thibault I, Siguret V, Gandrille S, Gaussem P, Le Bonniec B. FXa-alpha2-macroglobulin complex neutralizes direct oral anticoagulants targeting FXa in vitro and in vivo. *Thromb Haemost*. 2018;118:1535–44.

[32] Jourdi G, Abdoul J, Siguret V, Decleves X, Frezza E, Pailleret C, Gouin-Thibault I, Gandrille S, Neveux N, Samama CM, Pasquali S, Gaussem P. Induced forms of alpha(2)-macroglobulin neutralize heparin and direct oral anticoagulant effects. *Int J Biol Macromol*. 2021;184:209–17.

[33] Thalji NK, Ivanciu L, Davidson R, Gimotty PA, Krishnaswamy S, Camire RM. A rapid pro-hemostatic approach to overcome direct oral anticoagulants. *Nat Med*. 2016;22:924–32.

[34] Toso R, Zhu H, Camire RM. The conformational switch from the factor X zymogen to protease state mediates exosite expression and prothrombinase assembly. *J Biol Chem*. 2008;283:18627–35.

[35] Verhoef D, Visscher KM, Vosmeer CR, Cheung KL, Reitsma PH, Geerke DP, Bos MHA. Engineered factor Xa variants retain procoagulant activity independent of direct factor Xa inhibitors. *Nat Commun*. 2017;8:528.

[36] Higgins DL, Mann KG. The interaction of bovine factor V and factor V-derived peptides with phospholipid vesicles. *J Biol Chem*. 1983;258:6503–8.

[37] Toso R, Camire RM. Removal of B-domain sequences from factor V rather than specific proteolysis underlies the mechanism by which cofactor function is realized. *J Biol Chem*. 2004;279:21643–50.

[38] Camire RM, Larson PJ, Stafford DW, High KA. Enhanced gamma-carboxylation of recombinant factor X using a chimeric construct containing the prothrombin propeptide. *Biochemistry*. 2000;39:14322–9.

[39] Krishnaswamy S, Walker RK. Contribution of the prothrombin fragment 2 domain to the function of factor Va in the prothrombinase complex. *Biochemistry*. 1997;36:3319–30.

[40] Bos MH, Boltz M, St Pierre L, Masci PP, de Jersey J, Lavin MF, Camire RM. Venom factor V from the common brown snake escapes hemostatic regulation through procoagulant adaptations. *Blood*. 2009;114:686–92.

[41] Peraramelli S, Thomassen S, Heinzmann A, Hackeng TM, Hartmann R, Scheiflinger F, Dockal M, Rosing J. Role of exosite binding modulators in the inhibition of Fxa by TFPI. *Thromb Haemost*. 2016;115:580–90.

[42] Case DA, Cheatham TE 3rd, Darden T, Gohlke H, Luo R, Merz KM Jr, Onufriev A, Simmerling C, Wang B, Woods RJ. The Amber biomolecular simulation programs. *J Comput Chem*. 2005;26:1668–88.

[43] Case DA, Belfon K, Ben-Shalom IY, Brozell SR, Cerutti DS, Cheatham TE, Cruzeiro VWD, Darden TA, Duke RE, Giambasu G, Gilson MK, Gohlke H, Goetz AW, Harris S, Izadi S, Izmailov SA, Kasavajhala K, Kovalenko A, Krasny R, Kurtzman T, et al. *AMBER 2020*. San Francisco: University of California; 2020.

[44] Roe DR, Cheatham TE 3rd. PTRAJ and CPPTRAJ: software for processing and analysis of molecular dynamics trajectory data. *J Chem Theory Comput*. 2013;9:3084–95.

[45] Genheden S, Ryde U. The MM/PBSA and MM/GBSA methods to estimate ligand-binding affinities. *Expert Opin Drug Discov*. 2015;10:449–61.

[46] Miller BR 3rd, McGee TD Jr, Swails JM, Homeyer N, Gohlke H, Roitberg AE. MMPBSA.py: an efficient program for end-state free energy calculations. *J Chem Theory Comput*. 2012;8:3314–21.

[47] Pryzdial EL, Kessler GE. Kinetics of blood coagulation factor Xa alpha autoproteolytic conversion to factor Xabeta. Effect on inhibition by antithrombin, prothrombinase assembly, and enzyme activity. *J Biol Chem*. 1996;271:16621–6.

[48] Bos MHA, van 't Veer C, Reitsma PH. Molecular biology and biochemistry of the coagulation factors and pathways of hemostasis. In: Kaushansky K, Lichtman MA, Prchal JT, Levi MM, Burns LJ, Linch DC, eds. *Williams Hematology*. 10th edition. McGraw Hill Education; 2021:2017–50.

[49] Douxfils J, Adcock DM, Bates SM, Favaloro EJ, Gouin-Thibault I, Guillermo C, Kawai Y, Lindhoff-Last E, Kitchen S, Gosselin RC. 2021 update of the International Council for Standardization in Haematology recommendations for laboratory measurement of direct oral anticoagulants. *Thromb Haemost*. 2021;121:1008–20.

[50] Lu G, Broze GJ Jr, Krishnaswamy S. Formation of factors IXa and Xa by the extrinsic pathway: differential regulation by tissue factor pathway inhibitor and antithrombin III. *J Biol Chem*. 2004;279:17241–9.

[51] Zur M, Nemerson Y. Kinetics of factor IX activation via the extrinsic pathway. Dependence of Km on tissue factor. *J Biol Chem*. 1980;255:5703–7.

[52] Parasrampuria DA, Truitt KE. Pharmacokinetics and pharmacodynamics of edoxaban, a non-vitamin K antagonist oral anticoagulant that inhibits clotting factor Xa. *Clin Pharmacokinet*. 2016;55:641–55.

[53] Mueck W, Stampfuss J, Kubitza D, Becka M. Clinical pharmacokinetic and pharmacodynamic profile of rivaroxaban. *Clin Pharmacokinet*. 2014;53:1–16.

[54] Byon W, Garonzik S, Boyd RA, Frost CE. Apixaban: a clinical pharmacokinetic and pharmacodynamic review. *Clin Pharmacokinet*. 2019;58:1265–79.

[55] Yan VKC, Li HL, Wei L, Knapp MRJ, Wong ICK, Chan EW. Evolving trends in consumption of direct oral anticoagulants in 65 countries/regions from 2008 to 2019. *Drugs*. 2023;83:315–40.

[56] Hunter JD. Matplotlib: a 2D graphics environment. *Comput Sci Eng*. 2007;9:90–5.

[57] Renatus M, Bode W, Huber R, Sturzebecher J, Prasa D, Fischer S, Kohnert U, Stubbs MT. Structural mapping of the active site specificity determinants of human tissue-type plasminogen activator. Implications for the design of low molecular weight substrates and inhibitors. *J Biol Chem*. 1997;272:21713–9.

[58] Olson ST, Swanson R, Raub-Segall E, Bedsted T, Sadri M, Petitou M, Herault JP, Herbert JM, Bjork I. Accelerating ability of synthetic oligosaccharides on antithrombin inhibition of proteinases of the clotting and fibrinolytic systems. Comparison with heparin and low-molecular-weight heparin. *Thromb Haemost*. 2004;92:929–39.

[59] Camire RM. Prothrombinase assembly and S1 site occupation restore the catalytic activity of FXa impaired by mutation at the sodium-binding site. *J Biol Chem*. 2002;277:37863–70.

[60] Li W, Johnson DJ, Esmon CT, Huntington JA. Structure of the antithrombin-thrombin-heparin ternary complex reveals the antithrombotic mechanism of heparin. *Nat Struct Mol Biol*. 2004;11:857–62.

[61] Johnson DJ, Li W, Adams TE, Huntington JA. Antithrombin-S195A factor Xa-heparin structure reveals the allosteric mechanism of antithrombin activation. *EMBO J*. 2006;25:2029–37.

[62] Dahlback B, Tran S. The preAR2 region (1458-1492) in factor V-short is crucial for the synergistic TFPIα-cofactor activity with protein S and the assembly of a trimolecular factor Xa-inhibitory complex comprising FV-Short, protein S, and TFPIα. *J Thromb Haemost*. 2022;20:58–68.

[63] van Veen JJ, Gatt A, Makris M. Thrombin generation testing in routine clinical practice: are we there yet? *Br J Haematol*. 2008;142:889–903.

[64] Hertzberg M. Biochemistry of factor X. *Blood Rev*. 1994;8:56–62.

[65] Shapiro AD, Angchaisuksiri P, Astermark J, Benson G, Castaman G, Chowdary P, Eichler H, Jimenez-Yuste V, Kavakli K, Matsushita T, Poulsen LM, Wheeler AP, Young G, Zupancic-Salek S, Oldenburg J. Subcutaneous concizumab prophylaxis in hemophilia A and

hemophilia A/B with inhibitors: phase 2 trial results. *Blood*. 2019;134:1973–82.

[66] Hilden I, Lauritzen B, Sorensen BB, Clausen JT, Jespersgaard C, Krogh BO, Bowler AN, Breinholt J, Gruhler A, Svensson LA, Petersen HH, Petersen LC, Balling KW, Hansen L, Hermit MB, Egebjerg T, Friederichsen B, Ezban M, Bjorn SE. Hemostatic effect of a monoclonal antibody mAb 2021 blocking the interaction between FXa and TFPI in a rabbit hemophilia model. *Blood*. 2012;119:5871–8.

[67] Waters EK, Sigh J, Friedrich U, Hilden I, Sorensen BB. Concizumab, an anti-tissue factor pathway inhibitor antibody, induces increased thrombin generation in plasma from haemophilia patients and healthy subjects measured by the thrombin generation assay. *Haemophilia*. 2017;23:769–76.

[68] Broze GJ Jr, Girard TJ. Tissue factor pathway inhibitor: structure-function. *Front Biosci (Landmark Ed)*. 2012;17:262–80.

[69] Wood JP, Ellery PE, Maroney SA, Mast AE. Biology of tissue factor pathway inhibitor. *Blood*. 2014;123:2934–43.

[70] Qu SY, Xu Q, Wu W, Li F, Li CD, Huang R, Ding Q, Wei DQ. An unexpected dynamic binding mode between coagulation factor X and rivaroxaban reveals importance of flexibility in drug binding. *Chem Biol Drug Des*. 2019;94:1664–71.

[71] Krishnaswamy S. Exosite-driven substrate specificity and function in coagulation. *J Thromb Haemost*. 2005;3:54–67.

[72] Schreuder M, Poenou G, Strijbis VJF, Cheung KL, Reitsma PH, Bos MHA. Evolutionary adaptations in Pseudonaja textilis venom factor X induce zymogen activity and resistance to the intrinsic tenase complex. *Thromb Haemost*. 2020;120:1512–23.

[73] Lu G, Pine P, Leeds JM, DeGuzman F, Pratikhya P, Lin J, Malinowski J, Hollenbach SJ, Curnutte JT, Conley PB. Andexanet alfa effectively reverses edoxaban anticoagulation effects and associated bleeding in a rabbit acute hemorrhage model. *PLoS One*. 2018;13:e0195122.

[74] von Drygalski A, Bhat V, Gale AJ, Averell PM, Cramer TJ, Elias DJ, Griffin JH, Mosnier LO. An engineered factor Va prevents bleeding induced by direct-acting oral anticoagulants by different mechanisms. *Blood Adv*. 2020;4:3716–27.

[75] Verhoef D, Tjalma AVR, Cheung KL, Reitsma PH, Bos MHA. Elevated anti-human factor Xa activity in rabbit and rodent plasma: implications for preclinical assessment of human factor X in animal models of hemostasis. *Thromb Res*. 2021;198:154–62.

[76] Maroney SA, Ferrel JP, Pan S, White TA, Simari RD, McVey JH, Mast AE. Temporal expression of alternatively spliced forms of tissue factor pathway inhibitor in mice. *J Thromb Haemost*. 2009;7:1106–13.

[77] Siegal DM, Curnutte JT, Connolly SJ, Lu G, Conley PB, Wiens BL, Mathur VS, Castillo J, Bronson MD, Leeds JM, Mar FA, Gold A, Crowther MA. Andexanet alfa for the reversal of factor Xa inhibitor activity. *N Engl J Med*. 2015;373:2413–24.

[78] Menegatti M, Peyvandi F. Factor X deficiency. *Semin Thromb Hemost*. 2009;35:407–15.

SUPPLEMENTARY MATERIAL

The online version contains supplementary material available at https://doi.org/10.1016/j.jtha.2024.04.022